Stratified ACO-OFDM Modulation for Simultaneous Transmission of Multiple Frames Both on Even and Odd Subcarriers

Zelalem Hailu[1], Kibet Langat[2], and Ciira Maina[3]
[1] Pan African University Institute of Science, Technology and Innovation, Nairobi, Kenya
[2] Jomo Kenyatta University of Agriculture and Technology, Nairobi, Kenya
[3] Dedan Kimathi University of Technology, Nyeri, Kenya
Email: zelalembet@yahoo.com; kibetlp@jkuat.ac.ke; cwamaina.dekut@gmail.com

Abstract —Different variants of optical orthogonal frequency divisions multiplexing (O-OFDM) have been proposed for intensity modulation/direct detection (IM/DD) based indoor optical wireless communication. Among those schemes, direct current biased optical OFDM (DCO-OFDM) and asymmetrically clipped optical OFDM (ACO-OFDM) are widely adopted variants. These schemes have either reduced spectral or power efficiencies, but the co-existence of both good spectral and power efficiency is vital to tackle the challenge of limited bandwidth and limited optical power constraint scenarios. In this paper, simultaneous transmission of Multiple ACO-OFDM frames on both even and odd subcarriers has been proposed to achieve better spectral and energy efficiencies. The analysis of the theoretical bit error rate (BER) performance of the proposed scheme has been done and compared with the result from Monte Carlo simulation for Additive white Gaussian noise (AWGN) channel environment. A good agreement has been achieved between the theoretical BER bound and the simulated BER from Monte Carlo simulation. The proposed scheme provides better spectral efficiency (SE) compared to ACO-OFDM and equivalent SE compared to DCO-OFDM. In addition, it has shown superior energy efficiency performance than both ACO-OFDM and DCO-OFDM of equal SE.

Index Terms—Asymmetrically clipped optical OFDM (ACO-OFDM), direct current biased optical OFDM (DCO-OFDM), optical wireless communication, Intensity Modulation/Direct Detection (IM/DD).

I. Introduction

In the past few decades, the demand of wireless technologies has been increasing year by year. Smart electronic apparatuses which can support a number of multimedia applications have been common in our daily life. The benefit of having mobility feature and reduced cost keeps wireless communication technology at the forefront in telecommunication industry. The RF technology has been popular for many years for handling the wireless communication, but since the number of subscription and applications over RF is increasing year by year, the RF spectrum has been overcrowded by different applications and users including machines and humans. So that the RF band is almost exhausted and interference from so many applications becomes a big challenge. One of the most promised option which has wide unregulated bandwidth as a potential complement of RF technology is optical wireless communication. The optical spectrum, both visible and invisible, intended for this application can offer several thousand times higher bandwidth compared to RF spectrum. Moreover, optical wireless communication has high immunity for electromagnetic interference and excellent security features since it cannot penetrate walls. In recent years, solid state lightings based on white Light Emitting Diodes (LEDs) for illumination purpose to light our homes, cars, streets, stadiums, airplanes, and others are becoming more popular from time to time. This creates a huge motivation towards visible light to realize energy efficient high speed communication along with the illumination purpose at the same time. Due to the nature of LED used in the front end device, intensity modulation and direct detection (IM/DD) technique is confirmed as the most suitable scheme.

Orthogonal Frequency Division Multiplexing (OFDM) is considered as more suitable type of modulation scheme due to its ability of combating inter symbol interference (ISI) and its simple feature to use single-tap equalizer at the receiver. In practice, the well confirmed efficient way to realize OFDM is by using inverse Fast Fourier Transform (IFFT) at the transmitter and Fast Fourier Transform (FFT) at the receiver [1], [2].

The conventional OFDM signal is bipolar and complex valued but the use of IM/DD in optical wireless communication (OWC) needs the OFDM signal to be real valued and positive unipolar. This introduces a significant limitation on the system performance [3]. In the current state of the arts optical OFDM (O-OFDM) families, imposing Hermatian symmetry on subcarriers is used as a strategy to generate real valued bipolar time domain OFDM signal [1], [4], [5]. There are two general pioneer approaches to obtain a non-negative unipolar signal in M-QAM O-OFDM. The first one is direct current biased O-OFDM (DCO-OFDM) [2], [6] and the second technique includes generation of unipolar half Gaussian OFDM signals which is known as asymmetrically clipped O-OFDM (ACO-OFDM) [4], [7].

Manuscript received January 19, 2017; revised May 30, 2017.
Corresponding author email: zelalembet@yahoo.com.
doi:10.12720/jcm.12.5.261-270

©2017 Journal of Communications

DCO-OFDM is realized by adding a positive DC bias, defined as k on equation (1), on the bipolar OFDM signal. This is the easiest and straight forward technique for altering a bipolar signal into a unipolar positive signal. OFDM signal has well known characteristics of having high peak to average power (PAPR) ratio. So that, some samples will still be in the negative region even after adding the DC bias. The clipping of those negative samples which are left in the negative region introduce a distortion on the information. The optimum DC bias is different for different level M-QAM modulation and it is the multiple of the standard deviation of the signal at the output of IFFT module. Compared to bipolar OFDM signal, the increment of the dissipated electrical power B_{DC}^{dB} in DCO-OFDM due to the added DC bias can be written as [7]

$$B_{DC}^{dB} = 10\log_{10}(k^2+1) \tag{1}$$

The addition of DC bias on the bipolar OFDM signal reduces the energy efficiency and makes DCO-OFDM energy inefficient scheme. The spectral efficiency Se_{DCO} of DCO-OFDM for N available subcarriers is given by

$$Se_{DCO} = \frac{(\log_2 M)(N-2)}{2(N+N_{CP})} \quad . \tag{2}$$

On equation (2), M and N_{CP} are the level of QAM modulation used and the number of cyclic prefix respectively.

Unlike DCO-OFDM, ACO-OFDM avoids the DC biasing and generates a positive unipolar OFDM signal by exploiting the property of Fourier transform [4]. ACO-OFDM utilizes either odd or even subcarriers for information transmission. The conventional ACO-OFDM uses the odd subcarriers and wastes all the even subcarriers. The samples of the resulting time domain OFDM signal in conventional ACO-OFDM have the following relations [4].

$$x[n] = -x[n+\tfrac{N}{2}], \mathrm{n} = 0,1,...,\tfrac{N}{2}-1 \tag{3}$$

In ACO-OFDM which uses only odd subcarriers, the clipping of negative valued samples will not affect the odd subcarriers. The clipping noise totally falls on the even indexed subcarriers. But the power of the clipped signal is equal to half of the power of the bipolar signal since half of the signal power is lost due to the clipping process. If only the even subcarriers are used by leaving the odd subcarriers vacant, the samples of the time domain OFDM signal will have the following relationship.

$$x[n] = x[n+\tfrac{N}{2}], n = 0,1,2,...,\tfrac{N}{2}-1 \tag{4}$$

The spectral efficiency Se_{ACO}^{odd} of conventional ACO-OFDM which utilizes odd subcarriers can be written as the following formula.

$$Se_{ACO}^{odd} = \frac{(\log_2 M)(\mathrm{N})}{4(N+N_{CP})} \tag{5}$$

Similarly, the spectral efficiency Se_{ACO}^{even} of ACO-OFDM which utilizes only even subcarriers can be written as follows.

$$Se_{ACO}^{even} = \frac{(\log_2 M)(N-4)}{4(N+N_{CP})} \tag{6}$$

Even if ACO-OFDM avoids the DC bias and provides good energy efficiency, it is spectrally inefficient scheme since it wastes either the even or the odd subcarriers. Therefore, many significant efforts have been done on many literatures to enhance the performance of OFDM for OWC. Among those, Flip OFDM [8], unipolar OFDM (U-OFDM) [9], asymmetrically clipped DC-biased optical OFDM (ADO-OFDM) [10], and Enhanced Unipolar OFDM (eU-OFDM) [11] are proposed schemes. Recently, enhanced ACO-OFDM (eACO-OFDM) [12] which uses only odd subcarriers for transmission of multiple ACO-OFDM frames in stratified fashion and layered ACO-OFDM [13] which utilizes odd subcarrier on the first layer and even sub-carriers on the rest of the layers are proposed. In this paper, stratified architecture based simultaneous transmission of multiple ACO-OFDM frames on both even and odd subcarriers has been proposed to achieve better spectral and energy efficiencies in which even subcarriers are used in the first layer and odd subcarriers are used on the rest of the layers. Since the practical indoor optical wireless channel has low pass characteristics [14]-[16], including both even and odd subcarriers for data transmission provides fair number of channels in low frequency region and more bits can be loaded on those low frequency subcarriers during bit loading for improving the capacity of the system. The proposed transmission model combines multiple ACO-OFDM frames from odd and even subcarrier based ACO-OFDM modulators in to single time domain OFDM frame for simultaneous transmission. For Additive White Gaussian Noise (AWGN) channel environment, the performance comparison is done with ACO-OFDM and DCO-OFDM schemes.

The rest of this paper is organized as follows, in Section II, modulation /demodulation concept, spectral efficiency, electrical/optical power efficiencies, and theoretical BER bound of the proposed scheme will be discussed. In Section III, Monte Carlo simulation results and performance comparisons will be presented. Finally conclusions of the study will be made on Section IV.

II. The Proposed Scheme

A. Proposed Modulation Scheme

The proposed modulation scheme uses a layered O-OFDM modulation approach [11]-[13], [17]. As shown on Fig. 1, on contrary to layered ACO-OFDM [13] which utilizes odd subcarriers on the first layer and even

subcarriers on the rest of layers, the proposed stratified ACO-OFDM modulation scheme in this paper has S strata in which even subcarriers are utilized on the 1st stratum and odd subcarriers are utilized on the rest of $S-1$ strata. As confirmed on equations (5) and (6), utilizing odd subcarriers on $S-1$ strata has a benefit of utilizing one more subcarriers for data transmission at each stratum (ranging from the 2nd to the S^{th} stratum) compared to Layered ACO-OFDM proposed at [13]. As presented on Fig. 2, the arrangement and design of frames at each stratum is done in such a way that the clipping noise and the inter stream interference do not affect the subsequent stratum's information signal recovery at the receiver end. On this paper, Sub frames (SF) are used to represent half of ACO-OFDM frame. First half of the whole ACO-OFDM frame at any stratum is considered to be the first sub frame and the second half to be the second sub frame. At the 1st stratum, the length of the OFDM frame is chosen to be N and the signal generation is based on even subcarrier based ACO-OFDM modulator followed by modifications on the output time domain signal as shown in Fig. 1. As presented on Fig. 1, the output real bipolar OFDM signal $x_1[n]$ at the 1st stratum has the property given at equation (4). Before clipping the negative samples to obtain positive unipolar signals, the second sub frame is multiplied by -1 to flip the negative samples in to positive and the positive samples to negative. Let $x_{11}[n]$ and $x_{12}[n]$ are the 1st and 2nd sub frames at the first stratum after flipping is performed on the second sub frame. The two sub-frames can be given as

$$x_{11}[n] = x_1[n], n = 0,1,2,...,\tfrac{N}{2}-1 \quad (7)$$

and

$$x_{12}[n] = -x_1[n+\tfrac{N}{2}], n = 0,1,2,...,\tfrac{N}{2}-1 \quad (8)$$

After performing clipping of negative samples and addition of cyclic prefix (CP) on both $x_{11}[n]$ and $x_{12}[n]$, we will have unipolar sub-frames $x_{11}^{'}[n]$ and $x_{12}^{'}[n]$ respectively at the 1st stratum. This signal processing strategy at the 1st stratum provides a frame work to recover the clipped negative samples from the second sub frame of the transmitted signal at the receiver. Compared to the flipping technique used in Flip-OFDM [8] and eU-OFDM [11] which use two OFDM frames duration to transmit the complete information of one OFDM symbol, the flipping strategy used on this proposed scheme at the 1st stratum transmits the complete information of one OFDM symbol in one OFDM frame duration which has an importance of reducing latency compared to eU-OFDM. In Flip-OFDM and eU-OFDM, both the positive and the negative frames should be received in two frames duration to recover the information carried by single OFDM symbol, whereas the complete information of one OFDM symbol can be received in one frame duration for the case of the proposed scheme on this paper. In addition, for achieving good and simple equalization for multipath fading channel in FLIP-OFDM and eU-OFDM, the channel state should be unchanged in two OFDM frames durations, but in this proposed scheme equalization can be done easily and successfully as long as the channel state is unchanged with in one OFDM frame's duration. So that, this proposed scheme can be functional even at rapidly changing channel sates. At the rest of strata, the generation of signal is based on conventional ACO-OFDM modulator using odd sub-carriers. At the 2nd stratum, the length of the OFDM frame is equal to $\frac{N}{2}$ and it is replicated one time to obtain two exact copies. For the purpose of preserving the overall energy of the two copies and to equalize their energy with the energy of the original entire frame at the 2nd stratum, both copies are scaled by a factor $\frac{1}{\sqrt{2}}$ and CP is added on both copies [11]. After clipping the negative samples two unipolar sub frames $x_{21}^{'}[n]$ and $x_{22}^{'}[n]$ are obtained at the 2nd stratum. At the 3rd stratum, the original frame length is set to be $\frac{1}{4}$ and the generated signal is replicated to form 4 exact copies and each copy is scaled by a factor $\frac{1}{2}$ for equal symbol energy preservation. A pair of copies is merged together to form two new sub frames with length $\frac{N}{2}$ from the 4 regenerated copies. After adding CP and performing clipping of negative samples, the two positive unipolar sub frames, $x_{31}^{'}[n]$ and $x_{32}^{'}[n]$, are obtained at the 3rd stratum. Similarly, at any s^{th} stratum, $N/2^{s-1}$ length time domain signal is generated by conventional ACO-OFDM modulator, scaled by a factor $1/\sqrt{2^{s-1}}$, and replicated 2^{s-1}. After adding CP and clipping negative samples, enough number of replicated copies are merged together to form two sub frames having a length of $\frac{N}{2}$ each. As presented on Fig. 2 and Fig. 3, the 1st sub frames with length $\frac{N}{2}$ from all strata ($x_{11}^{'}[n], x_{21}^{'}[n], x_{31}^{'}[n], ..., x_{S1}^{'}[n]$) are added to form the first sub frame $x_{t1}[n]$ of the combined signal. In the same way $x_{11}^{'}[n], x_{21}^{'}[n], x_{31}^{'}[n], ..., x_{S1}^{'}[n]$ are combined to form the 2nd combined sub frame $x_{t2}[n]$. The first and the second sub frames of the combined signal, $x_{t1}[n]$ and $x_{t2}[n]$ respectively, are transmitted separately one after another during transmission. Therefore, the entire frame of the proposed stratified ACO-OFDM modulation scheme is transmitted in two consecutive transmission phases as shown on Fig. 2 (b).

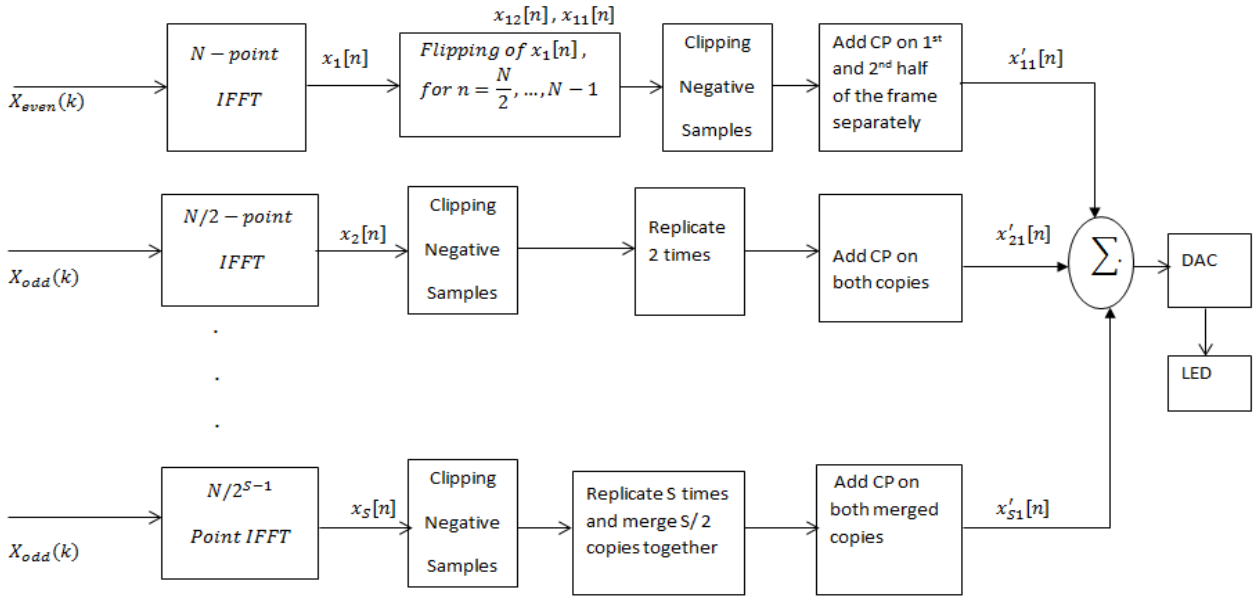

Fig. 1. Block diagram of the proposed stratified ACO-OFDM with S strata where $X_{even}[k]$ and $X_{odd}[k]$ are the M-QAM symbols loaded on even and odd sub-carriers respectively.

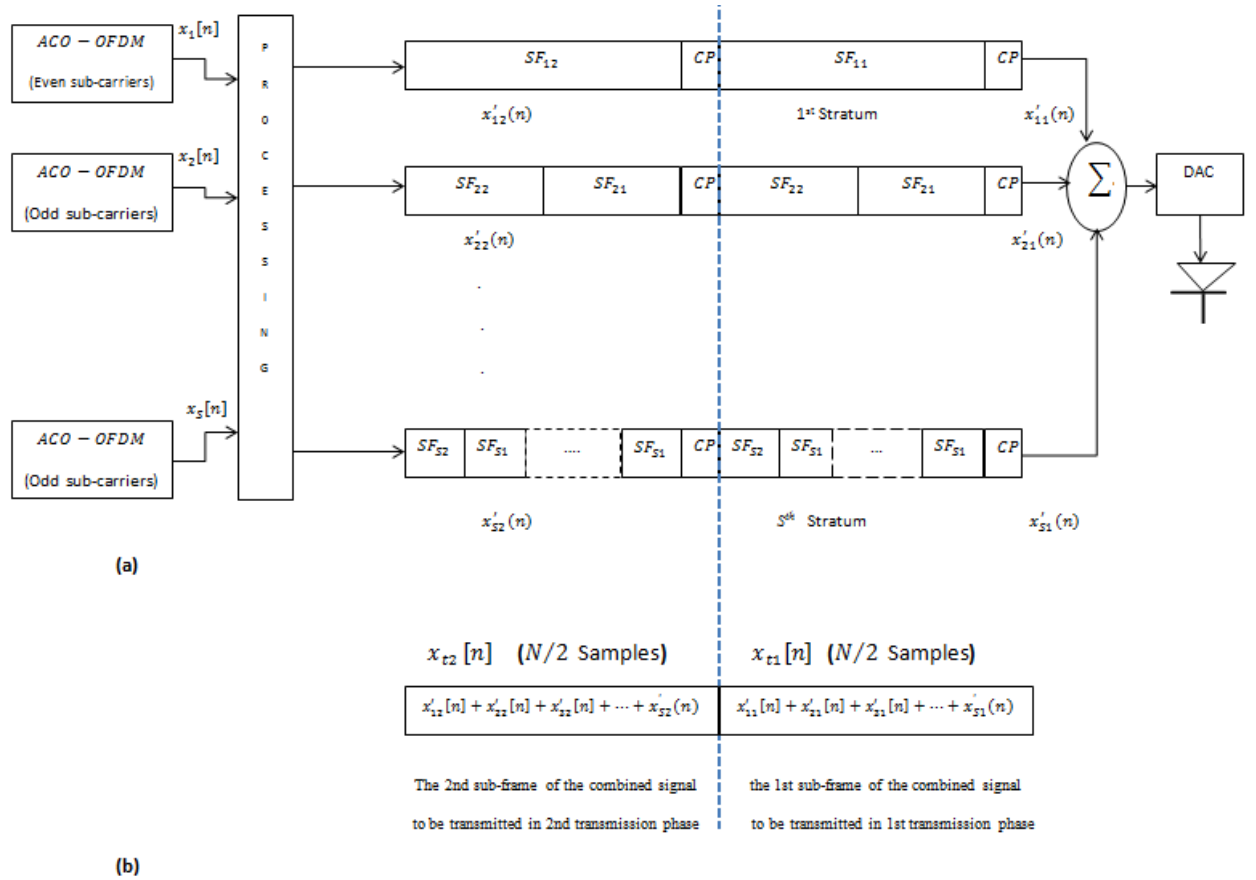

Fig. 2. Arrangement of frames at each stratum of the proposed modulation scheme, (a) the representation SF_{s1} and SF_{s2} stand for the 1st and the 2nd original sub frames of s^{th} stratum respectively. (b) The first and the second combined sub frames to be transmitted in two consecutive transmission sessions

B. Demodulation Scheme

Let $x_{r1}[n]$ and $x_{r2}[n]$ are first and the second received sub frames of the combined signal at the receiver from the two consecutive transmission phases which can be written as [4]

$$x_{r1}(t) = h(t) * x_{t1}(t) + z(t) \quad (9)$$

and

$$x_{r2}(t) = h(t) * x_{t2}(t) + z(t)\,. \quad (10)$$

where x_{t1}(t) and x_{t2}(t) are the analog versions of the transmitted sub frames $x_{t1}[n]$ and $x_{t2}[n]$ respectively, $h(t)$ is the channel impulse response, and z(t) is the additive white Gaussian noise. If pure AWGN channel environment is considered, the received signals at the output of analog to digital converter (ADC) of the receiver become

$$\begin{aligned} x_{r1}[n] &= x_{t1}[n] + z[n], \mathrm{n} = 0,1,...,\tfrac{N}{2}-1 \\ &= x_{11}^{'}[n] + x_{21}^{'}[n] + ... + x_{S1}^{'}[n] + z[n] \end{aligned} \quad (11)$$

and

$$\begin{aligned} x_{r2}[n] &= x_{t2}[n] + z[n], \mathrm{n} = 0,1,...,\tfrac{N}{2}-1 \\ &= x_{12}^{'}[n] + x_{22}^{'}[n] + ... + x_{S2}^{'}[n] + z[n]\,. \end{aligned} \quad (12)$$

In equations (11) and (12), $z[n]$ are the respective AWGN samples in one sub frame duration. After removing the cyclic prefixes from $x_{r1}[n]$ and $x_{r2}[n]$, the demodulation process is begin by subtracting $x_{r2}[n]$ from $x_{r1}[n]$ to get $x_d[n]$ as follows.

$$x_d[n] = x_{r1}[n] - x_{r2}[n], n = 0,1,2,...,\tfrac{N}{2}-1 \quad (13)$$

Due to the subtraction process, the signals of the higher strata are vanished and only the first original bipolar sub-frame of the first stratum with AWGN noise is left as

$$x_d[n] = x_1[n] + z^{'}[n], n = 0,1,2,...,\tfrac{N}{2}-1 \quad (14)$$

As presented in equation (14), the inter-frame interferences and the clipping noise due to higher strata's streams are also vanished in the process of subtraction. $z^{'}[n]$ in equation (14) represent the new AWGN noise samples after subtraction. If we ignore $z^{'}[n]$ from equation (14) without loss of generality, we will have

$$x_d[n] = x_1[n] = x_1[n + \tfrac{N}{2}], n = 0,1,2,...,\tfrac{N}{2}-1 \quad (15)$$

The complete information carried on the 1st stratum can be obtained by padding $\frac{N}{2}$ zeros at the end of $x_d[n]$. After zero padding at the end of $x_d[n]$, the resulted signal $x_1^{zp}[n]$ is given by

$$x_1^{zp}[n] = \begin{cases} x_1[n] = x_d[n], n = 0,1,...,\tfrac{N}{2}-1 \\ 0, n = \tfrac{N}{2}, \tfrac{N}{2}+1, ..., N-1 \end{cases} \quad (16)$$

Finally, the information carried by the 1st stratum will be recovered from even subcarriers by demodulating $x_1^{zp}[n]$ with ACO-OFDM demodulator. The zero level clipping introduced by zero padding on the second half of $x_1[n]$ results in a clipping noise on odd subcarriers while the even subcarriers are unaffected by clipping noise. But the amplitude of the received signal on even subcarriers is reduced by half compared to the transmitted signal because of the clipping. After demodulating 1st stratum information, the time domain signal of 1st stratum is then reconstructed at the receiver by re-modulating the recovered bits, and then it is subtracted from the respective $x_{r1}[n]$ and $x_{r2}[n]$ to remove the contribution of the 1st stratum from the combined signal. While removing the contribution of the 1st stratum, the clipping noise on odd subcarriers due to the 1st stratum stream will also be vanished. The information carried at the 2nd stratum can be recovered from odd subcarriers by summing the two similar sub frames left after removing the contribution of the 1st stratum and demodulating the resulting signal using conventional ACO-OFDM demodulator. The clipping noise and inter-frame interference due to higher strata's frames are falling on the even subcarriers but it has no any effect on the system performance since the information of the 1st stratum is already recovered from even subcarriers. In similar way, the stream at the 2nd stratum is reconstructed again at the receiver. The entire frame at the 3rd stratum can be obtained by subtracting 2nd stratum stream from the combined signal left after the removal of 1st stratum stream. After summing the four similar copies, the information carried by the 3rd stratum can be recovered from odd subcarriers using ACO-OFDM demodulator. By performing the same process, the information carried by each stratum can be recovered successively. During the successive demodulation, residual errors are propagating from lower stratum to higher stratum in downward direction.

C. Spectral Efficiency

The spectral efficiency $Se(S)$ of the proposed scheme is equal to the summation of spectral efficiencies provided by each stratum as [17], [11]

$$Se(S) = \sum\nolimits_s Se_s, s = 1,2,...,S \quad (17)$$

where Se_s is the spectral efficiency of the s^{th} stratum and given by [12]

$$Se_s = \frac{(\log_2 M_S)(\mathrm{N}_s)}{4(\mathrm{N} + \mathrm{N}_{CP})} \quad (18)$$

In the above equation, N_s and M_s are stand for the number of information carrying subcarriers and the level of QAM modulation used at the s^{th} stratum respectively. For the same M-QAM modulations used, the proposed scheme has equivalent spectral efficiency to eU-OFDM and DCO-OFDM and better spectral efficiency compared to ACO-OFDM. In addition, if more than 2 strata are used, the proposed scheme provides better spectral efficiency compared to SEE-OFDM [18]. Fig. 3 shows

the spectral efficiency comparisons among DCO-OFDM, ACO-OFDM and the proposed scheme for 16-QAM modulation at each stratum.

D. Electrical Power Efficiency

The average electrical power P_e^{avg} of the entire transmitted signal $x_t(t)$ at the output of digital to analog converter (DAC) of the transmitter for one OFDM frame can be calculated from the average power of the two transmitted sub frames $x_{t1}(t)$ and $x_{t2}(t)$ as it is given by the following formula [7], [17].

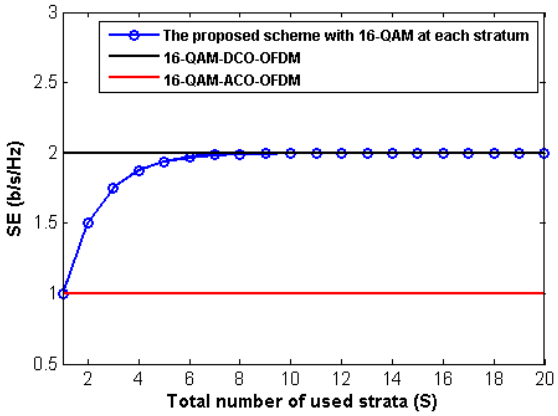

Fig. 3. Spectral efficiency comparison for proposed scheme, DCO-OFDM, and ACO-OFDM

$$\begin{aligned} P_e^{avg} &= E[x_t^2(t)] \\ &= \tfrac{1}{2}(E[x_{t1}^2(t)+E[x_{t2}^2(t)) \\ &= \tfrac{1}{2}(E[(\sum_s x_{s1}^{'}(t))^2]+E[(\sum_s x_{s2}^{'}(t))^2]), s=1,2,3,...,S \end{aligned} \quad (19)$$

On equation (19), $x_{s1}^{'}(t)$ and $x_{s2}^{'}(t)$ are the contribution of s^{th} stratum for the transmitted sub frame signals $x_{t1}(t)$ and $x_{t2}(t)$ respectively. The derivation of equation (19) is given on the appendix (A-1 &A-2). The electrical signal to noise ratio (SNR) of this scheme γ based on energy per bit is [7], [17]

$$\gamma = \frac{E_b^e}{N_o} = \frac{P_e^{avg}}{BN_o(Se)} \quad (20)$$

where E_b^e, N_o and B are stand for electrical energy per bit, single sided power spectral density (PSD), and total employed bandwidth respectively. The average electrical power P_s^e of the signal at s^{th} stratum can be given by

$$P_s^e = \tfrac{1}{2}(E[(x_{s1}^{'})^2]+E[(x_{s2}^{'})^2]), s=1,2,...,S \quad (21)$$

The average power increment α_s due to the combination of signal from many strata in relative to the average power of the signal at s^{th} stratum is given by [7]

$$\alpha_s = \frac{P_e^{avg}}{P_s^e}, s=1,2,3,...,S \quad (22)$$

α_s can be interpreted as the SNR penalty introduced due to the combination of multiple streams while comparing the SNR of the entire system with the SNR of s^{th} stratum. The electrical SNR of the signal γ_s in terms of bit energy at s^{th} stratum can be defined as [7]

$$\gamma_s = \frac{E_s^b}{N_o} = \frac{P_s^e}{BN_o(Se_s)}, s=1,2,...,S \quad (23)$$

On equation (23) E_s^b stands for energy per bit at s^{th} stratum. Therefore, the increment of energy dissipation per bit μ_s for the combined system compared to the energy per bit of s^{th} is given by [17]

$$\mu_s = \frac{\gamma}{\gamma_s} = \alpha_s(\frac{Se_s}{Se}), s=1,2,...,S \quad (24)$$

E. Optical Power Efficiency

As shown on the appendix (A-3 & A-4), the average transmitted optical power P_o^{avg} of the proposed scheme is given by [7]

$$\begin{aligned} P_o^{avg} &= E[x_t(t)] \\ &= \tfrac{1}{2}(E[x_{t1}(t)+E[x_{t2}(t)) \\ &= \tfrac{1}{2}(E[\sum_s x_{s1}^{'}(t)]+E[\sum_s x_{s2}^{'}(t)]), s=1,2,...,S. \end{aligned} \quad (25)$$

The optical SNR γ_o of the proposed scheme in terms of optical energy per bit (E_b^o) is also given by [7]

$$\gamma_o = \frac{E_b^o}{N_o} = \frac{P_o^{avg}}{BN_o(Se)} \quad (26)$$

F. Theoretical BER Bound

The theoretical BER bound of each stratum can be derived from the BER formula of real bipolar M-QAM-OFDM [19] by accounting the SNR penalty introduced by the clipping and signal combination process. The achieved SNR at the receiver which is presented at equation (20) should be multiplied by a factor $\frac{1}{2\mu_s}$ to use the BER formula of bi-polar M-QAM-OFDM. The factor $\frac{1}{2}$ is penalty due to clipping while $\frac{1}{\mu_s}$ is the penalty due to the combination of signal from multiple strata. The theoretical BER bound BER_s at s^{th} stratum is defined as

$$\begin{aligned} BER_s &\cong BER_{QAM}(M_s, \tfrac{\gamma}{2\mu_s}) \\ &\cong \frac{4}{\log_2 M_s}(1-\frac{1}{\sqrt{M_s}})\sum_{i=1}^{\frac{\sqrt{M_s}}{2}}(Q((2i-1)\sqrt{\frac{3\log_2 M_s \gamma}{2\mu_s(M_s-1)}})) \end{aligned} \quad (27)$$

The theoretical BER bound of the proposed scheme can be obtained from the BER of each subsequent stratum. But since the number of transmitted bits at each stratum with in one frame duration is different, the percentage of contribution of BER from each stratum is different.

Let N_{tot}^{b}, N_{er}^{b} and N_{s}^{b} are the total number of bits carried by all strata, the total number of erroneous bits received on all strata, and total number of bits transmitted on s^{th} stratum over one transmission time respectively. The BER bound BER_c of the combined system over AWGN channel can be given by

$$BER_c = \frac{N_{tot}^{b}}{N_{er}^{b}} \cong \frac{\sum_{s=1}^{S}(BER_s N_s^b)}{\sum_{s=1}^{S} N_s^b} \quad (28)$$

where $N_s^b = N_s \log_2 M_s$ and N_s is the total number of information carrying sub carriers at s^{th} stratum. The BER formulas in equations (27) and (28) do not account the error propagation from lower stratum to higher stratum during the successive demodulation process.

III. Simulation Results

The BER performance of the proposed scheme is compared with the BER performance of DCO-OFDM and ACO-OFDM of equal spectral efficiencies. The optimal constellation size combination and the respective used scaling factors for the proposed scheme are similar to [7]. The performance of ACO-OFDM and DCO-OFDM used for comparisons in this paper are consistent with [17], [20]. The BER performance of each stratum of the proposed scheme is also compared with its theoretical BER bound. 2048 total sub carriers and 3 strata are used for simulation setup in AWGN channel environment. Fig. 4 Shows the BER performance at each stratum of the proposed scheme for SE of 2 bits/s/Hz. At the 1st stratum, the theoretical BER bound and the simulated BER are equal since the only source of error at the 1st stratum is AWGN noise. At the 2nd and 3rd strata, the theoretical BER is slightly less than the simulated BER because of the residual error propagated from stratum to stratum in downward direction during successive demodulation. The residual BER is not included in the theoretical BER formula given at equation (28). The residual errors propagating from stratum to stratum become negligible when the SNR of the system increases. Therefore, at the 2nd and 3rd strata, the theoretical and the simulated BER are going to approach each other while the SNR of the system is increased. Fig. 5, Fig. 6, and Fig. 7 show the comparisons of BER performance as a function of electrical SNR in dB for the proposed scheme, DCO-OFDM, and ACO-OFDM for similar spectral efficiencies of 1.5, 2, and 2.5 bits/s/Hz respectively. For spectral efficiency of 1.5 bits/s/Hz, 16-8-4-QAM-ACO-OFDM is used for the proposed scheme, meaning that, 16-QAM at 1st stratum, 8-QAM at 2nd stratum, and 4-QAM at 3rd stratum are used.

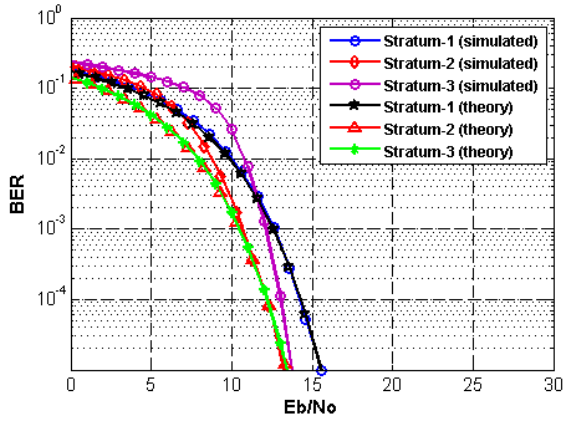

Fig. 4. BER versus electrical E_b/N_o of each stratum for the proposed scheme with SE= 2 bits/s/Hz (32-16-16 QAM).

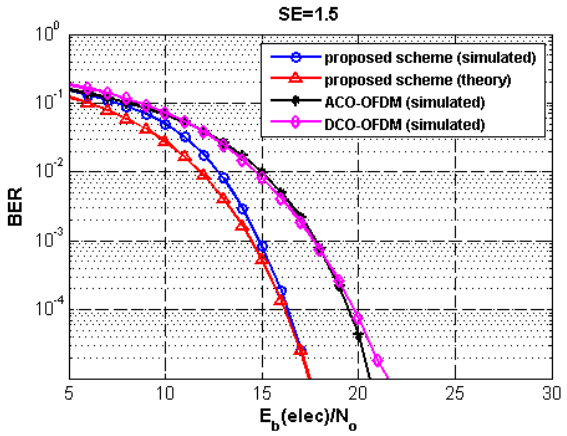

Fig. 5. BER versus electrical E_b/N_o for 16-8-4-QAM proposed scheme, 64-QAM ACO-OFDM, and 8-QAM DCO-OFDM, i.e. SE= 1.5 bits/s/Hz.

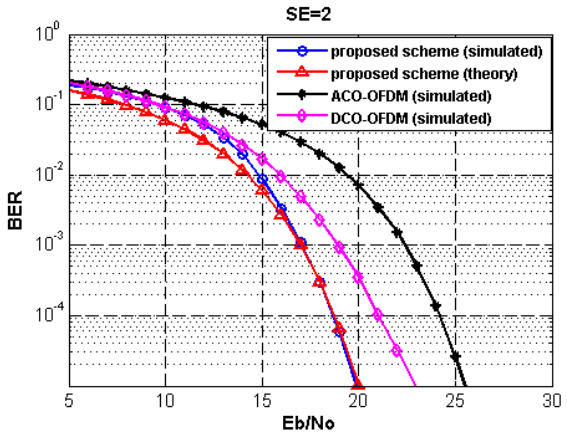

Fig. 6. BER versus electrical E_b/N_o for 32-16-16-QAM proposed scheme, 256-QAM ACO-OFDM, and 16-QAM DCO-OFDM, i.e. SE= 2 bits/s/Hz.

So that, 16-8-4-QAM-ACO-OFDM proposed scheme is compared with 64-QAM-ACO-OFDM and 8-QAM-DCO-OFDM with 7 dB DC-bias. As shown on Fig. 5 the BER performance of the proposed scheme shows better

performance with around 2.5dB electrical energy saving compared to ACO-OFDM and 3dB electrical energy savings compared to DCO-OFDM to achieve a BER of 10^{-5} for SE of 1.5 bits/s/Hz. For spectral efficiency of 2 bits/s/Hz, 32-16-16 QAM-ACO-OFDM proposed scheme is compared with 256-QAM ACO-OFDM and 16-QAM DCO-OFDM with 7.5 dB DC-bias. Again the proposed scheme shows better electrical energy saving which is about 2.5 dB compared to DCO-OFDM and 5.5 dB compared to ACO-OFDM to achieve a BER of 10^{-5} as presented on Fig. 6. For spectral efficiency of 2.5 bits/s/Hz, 64-64-16-QAM ACO-OFDM proposed scheme is compared with 1024-QAM ACO-OFDM and 32-QAM DCO-OFDM with 8 dB DC-bias as shown on Fig. 7. To achieve a BER of 10^{-5}, the proposed scheme shows around 2.5dB electrical energy savings compared to DCO-OFDM and 7.5dB electrical energy savings compared to ACO-OFDM scheme. For higher spectral efficiency, i.e. 2.5 bits/s/Hz, the BER performance gap between the proposed scheme and ACO-OFDM is wider. While increasing spectral efficiency, the SNR penalty of ACO-OFDM in relative to the proposed scheme will increase since higher level M-QAM modulation will be used in ACO-OFDM to fill the spectral efficiency gap.

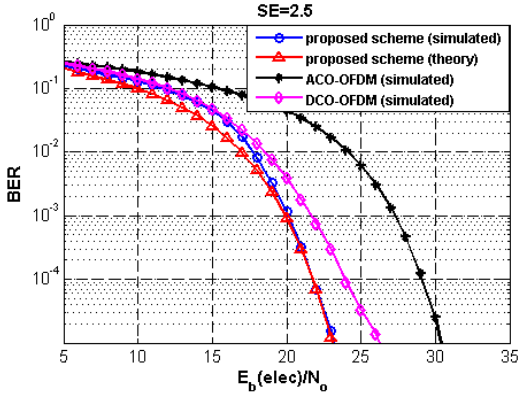

Fig. 7. BER versus electrical E_b/N_o for 64-64-16-QAM proposed scheme, 1024-QAM ACO-OFDM, and 32-QAM DCO-OFDM, i.e. SE= 2.5 bits/s/Hz.

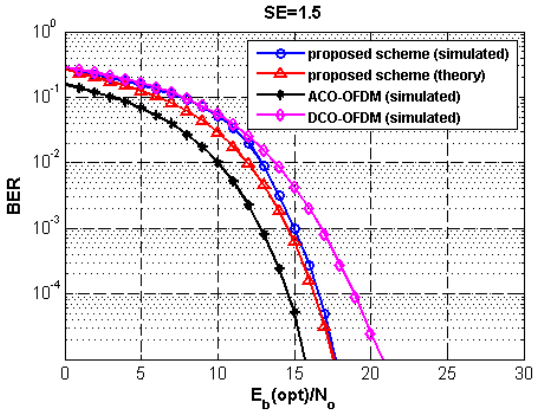

Fig. 8. BER versus optical E_b/N_o for 16-8-4-QAM proposed scheme, 64-QAM ACO-OFDM, and 8-QAM DCO-OFDM, i.e. SE= 1.5 bits/s/Hz.

In Fig. 8, Fig. 9, and Fig. 10, the BER performance of the three schemes as a function of optical energy per bit to noise power ratio ($E_{b(opt)}/N_o$) is presented.

The comparison is done by normalizing the optical power to unity for all the three schemes for fair comparisons. As shown on Fig. 8, for SE of 1.5 bits/s/Hz, the proposed scheme provides better optical energy efficiency compared to DCO-OFDM with optical energy saving of around 3.5dB to achieve a BER of 10^{-5}. But it has lower optical energy efficiency compared to ACO-OFDM at SE of 1.5 bits/s/Hz. For SE of 2 bits/s/Hz, the proposed scheme provides equivalent optical energy efficiency with ACO-OFDM. But compared to DCO-OFDM, it has shown superior optical energy efficiency with around 2.5dB optical energy saving to achieve a BER of 10^{-5} as shown on Fig. 9. For SE of 2.5 bits/s/Hz, the proposed scheme shows better performance with optical energy savings of 2dB to achieve a BER of compared to both ACO-OFDM and DCO-OFDM as presented on Fig. 10.

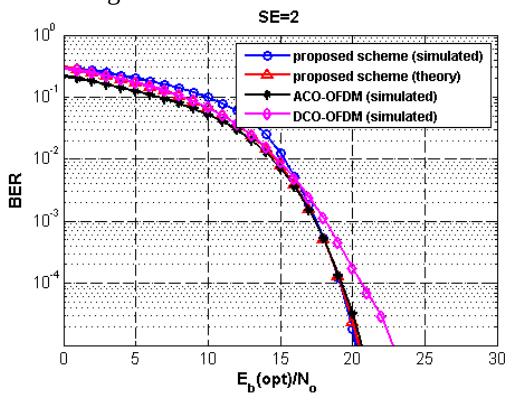

Fig. 9. BER versus optical E_b/N_o for 32-16-16-QAM proposed scheme, 256-QAM ACO-OFDM, and 16-QAM DCO-OFDM, i.e. SE= 2 bits/s/Hz.

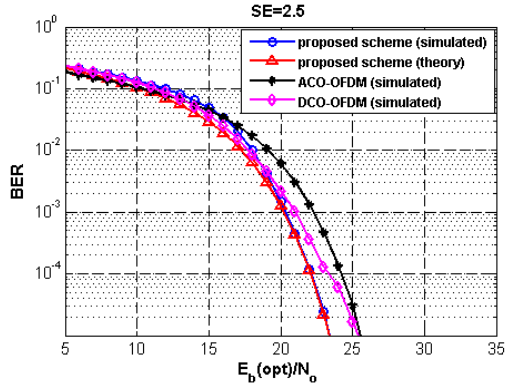

Fig. 10. BER versus optical E_b/N_o for 64-64-16-QAM proposed scheme, 1024-QAM ACO-OFDM, and 32-QAM DCO-OFDM, i.e. SE= 2.5 bits/s/Hz.

IV. Conclusion

A scheme which adopts a layered approach to transmit multiple ACO-OFDM frames simultaneously on even

sub-carriers at the first stratum and odd sub-carriers on the rest strata is proposed and presented. The spectral efficiency of the proposed scheme is better than ACO-OFDM and equivalent to DCO-OFDM. The theoretical BER bound and the simulated BER from Monte Carlo simulation have shown good agreement. For similar spectral efficiencies, the proposed scheme provides better energy efficiency compared to both ACO-OFDM and DCO-OFDM. The future research will focus on analyzing the performance of the proposed scheme in frequency selective multipath diffused optical channel and with Adaptive bit loading algorithms for different optical wireless channel dynamics.

APPENDIX

From Fig. 2 (b), the entire time domain OFDM frame $x_t(t)$ of the proposed scheme is composed of two sub frames which are $x_{t1}(t)$ and $x_{t2}(t)$. If the entire frame duration of one OFDM frame is T, then the duration of the first and the second sub-frames is equal to half of T. Therefore, $T_1 = T_2 = \frac{T}{2}$ where T_1 and T_2 are the duration of the first and second sub-frame respectively. The electrical average power of the two sub-frames can be given by

$$\begin{aligned} P_1^{avg} &= E[x_{t1}^2(t)] \\ &= \lim_{T_1\to\infty} \frac{1}{T_1}\int_0^{T_1} x_{t1}^2(t)dt \\ &= \lim_{T\to\infty} \frac{2}{T}\int_0^{\frac{T}{2}} x_{t1}^2(t)dt \end{aligned}$$

And

$$\begin{aligned} P_2^{avg} &= E[x_{t2}^2(t)] \\ &= \lim_{T_2\to\infty} \frac{1}{T_2}\int_0^{T_2} x_{t2}^2(t)dt \\ &= \lim_{T\to\infty} \frac{2}{T}\int_{\frac{T}{2}}^{T} x_{t2}^2(t)dt . \end{aligned} \quad \text{(A-1)}$$

where P_1^{avg} and P_2^{avg} are the average electrical power of the first and the second sub frames of the entire OFDM frame. The average electrical power of the complete transmitted OFDM frame P_e^{avg} is given by

$$\begin{aligned} P_e^{avg} &= E[x_t^2(t)] \\ &= \lim_{T\to\infty} \frac{1}{T}\int_0^{T} x_t^2(t)dt \\ &= \lim_{T\to\infty} \frac{2}{T}\int_0^{\frac{T}{2}} x_{t1}^2(t)dt + \lim_{T\to\infty} \frac{2}{T}\int_{\frac{T}{2}}^{T} x_{t2}^2(t)dt \\ &= \frac{1}{2}(E[x_{t1}^2(t) + E[x_{t2}^2(t)]) . \end{aligned} \quad \text{(A-2)}$$

Similarly the optical power of the two sub frames and the complete frame can be given by

$$\begin{aligned} P_1^o &= E[x_{t1}(t)] \\ &= \lim_{T_1\to\infty} \frac{1}{T_1}\int_0^{T_1} x_{t1}(t)dt \\ &= \lim_{T\to\infty} \frac{2}{T}\int_0^{\frac{T}{2}} x_{t1}(t)dt \end{aligned}$$

and

$$\begin{aligned} P_2^o &= E[x_{t2}(t)] \\ &= \lim_{T_2\to\infty} \frac{1}{T_2}\int_0^{T_2} x_{t2}(t)dt \\ &= \lim_{T\to\infty} \frac{2}{T}\int_{\frac{T}{2}}^{T} x_{t2}(t)dt \end{aligned} \quad \text{(A-3)}$$

where P_1^o and P_2^o are the average optical power of the first and the second sub-frames of the entire OFDM frame. The average optical power of the complete transmitted OFDM frame P_o^{avg} is given by

$$\begin{aligned} P_o^{avg} &= E[x_t(t)] \\ &= \lim_{T\to\infty} \frac{1}{T}\int_0^{T} x_t(t)dt \\ &= \lim_{T\to\infty} \frac{2}{T}\int_0^{\frac{T}{2}} x_{t1}(t)dt + \lim_{T\to\infty} \frac{2}{T}\int_{\frac{T}{2}}^{T} x_{t2}(t)dt \\ &= \frac{1}{2}(E[x_{t1}(t) + E[x_{t2}(t)]) . \end{aligned} \quad \text{(A-4)}$$

REFERENCES

[1] J. Armstrong, "OFDM for optical communications," *Journal of Light Wave Technology*, vol. 27, no. 3, pp. 189-204, February 2009.

[2] J. B. Carruthers and J. M. Kahn, "Multiple-subcarrier modulation for non-directed wireless infrared communication," *IEEE Journal on Selected Areas in Communications*, vol. 14, no. 3, pp. 538-546, April 1996.

[3] S. Dimitrov and H. Haas, *Principles of LED Light Communications: Towards Networked Li-Fi*, Cambridge University Press, 2015, ch. 4.

[4] J. Armstrong and A. Lowery, "Power efficient optical OFDM," *Electronics Letters*, vol. 42, no. 6, pp. 370-372, March 2006.

[5] K. K. Wong and T. O'Farrell, "Spread spectrum techniques for indoor wireless IR communications," *IEEE Wireless Communications*, vol. 10, no. 2, pp. 54-63, April 2003.

[6] T. Ohtsuki, "Multiple–Subcarrier modulation in optical wireless communications," *IEEE Communications Magazine*, vol. 41, no. 3, pp. 74-79, March 2003.

[7] J. Armstrong and B. J. C. Schmidt, "Comparison of asymmetrically clipped optical OFDM and DC-Based optical OFDM in AWGN," *IEEE Communications Letters*, vol. 12, no. 5, pp. 343-345, May 2008.
[8] N. Fernando, H. Yi, and E. Viterbo, "Flip-OFDM for unipolar communication systems," *IEEE Trans. Commun.*, vol. 60, no. 12, pp. 3726-3733, December 2012.
[9] D. Tsonev, S. Sinanovic, and H. Haas, "Novel unipolar orthogonal frequency division multiplexing (U-OFDM) for optical wireless," in *Proc. Vehicular Technology Conference*, Yokohama, Japan, 2012.
[10] S. D. Dissanayake and J. Armstrong, "Comparison of ACO-OFDM, DCO-OFDM and ADO-OFDM in IM/DD systems," *Journal of Light Wave Technology*, vol. 31, no. 7, pp. 1063-1072, April 2013.
[11] S. Videv, H. Haas, and D. Tsonev, "Unlocking spectral efficiency in intensity modulation and direct detection systems," *IEEE Journal on Selected Areas in Communications*, vol. 33, no. 9, pp. 1758-1770, September 2015.
[12] S. Islim, D. Tsonev, and H. Haas, "On the superposition modulation for OFDM-based optical wireless communication," in *Proc. IEEE Global Conference on Signal and Information Processing*, Orlando, Florida, USA, 2015, pp. 1022-1026.
[13] Q. Wang, C. Qian, X. Guo, Z. Wang, G. Cunningham, and H. White, "Layered ACO-OFDM for intensity-modulated direct-detection optical wireless transmission," *OSA*, vol. 23, no. 9, pp. 12382-12393, May 2015.
[14] K. Wilson and J. Armstrong, "Digital modulation techniques for optical asymmetrically-clipped OFDM," in *Proc. IEEE Wireless Communications and Networking Conference*, Las Vegas, USA, 2008, pp. 538-542.
[15] J. Grubor, V. Jungnickel, and K. D. Langer, "Capacity analysis in indoor wireless infrared communication using adaptive multiple subcarrier transmission," in *Proc. 7th International Conference on Transparent Optical Networks*, Barcelona, Spain, 2005, pp. 171-174.
[16] V. Jungnickel, V. Pohl, S. Nonnig, and C. von Helmolt, "A physical model of the wireless infrared communication channel," *IEEE Journal on Selected Areas in Communications*, vol. 20, no. 3, pp. 631-640, April 2002.
[17] M. Islim, D. Tsonev, and H. Haas, "A generalized solution to the spectral efficiency loss in unipolar optical OFDM-based systems," in *Proc. IEEE International Conference on Communications*, London, UK, 2015, pp. 5126-5131.
[18] H. Elgala and D. C. Little, "SEE-OFDM: Spectral and energy efficient OFDM for optical IM/DD systems," in *Proc. IEEE Personal, Indoor, and Mobile Radio Communication (PIMRC) Annual International Symposium*, Washington, DC, USA, 2014.
[19] F. Xiong, *Digital Modulation Techniques*, 2nd ed. Norwood, USA: Artech House, 2006, ch. 9.
[20] D. Dissanayake, K. Panta, and J. Armstrong, "A novel technique to simultaneously transmit ACO-OFDM and DCO-OFDM in IM/DD systems," in *Proc. IEEE GLOBECOM Workshops (GC Wkshps)*, Houston, Texas, USA, 2011, pp. 782-786.

Zelalem Hailu was born in Amhara region, Woreilu town, Ethiopia, in 1984. He is currently a PhD student in Electrical Engineering (Telecommunication option) at Pan African University Institute of Science, Technology and Innovation, Nairobi, Kenya. He received his B.Sc. degree in Electrical Engineering from Hawassa University, Ethiopia, in 2007 and M.Sc. degree in optical communication and photonic technologies from Politecnico di Torino, Italy, by the year 2012. His research interests include signal processing and OFDM modulation for optical wireless and optical fiber communications.

Kibet Langat received his PhD in Electronic Engineering from Stellenbosch University, South Africa. His research interests include wireless communication, applied electromagnetics, and multi-antenna communications and applications.

Ciira Maina received his PhD in Electrical and computer engineering from Drexel University in 2011. His research interests include wireless communication, Statistical signal processing for speech applications, and Computational Biology.